Frequency Dependency in UWB Channel Modelling

Wen Zhang
Faculty of Engineering and IT
Australian National University
Canberra ACT 0200 Australia
Email: u2580470@anu.edu.au

Thushara D. Abhayapala
Wireless Signal Process Program
National ICT Australia
Canberra ACT 2601, Australia
Email: Thushara.Abhayapala@nicta.com.au

Jian Zhang
Wireless Signal Process Program
National ICT Australia
Canberra ACT 2601, Australia
Email: Andrew.Zhang@nicta.com.au

***Abstract*— This paper presents a novel parametric Ultra-wideband (UWB) channel model to characterize frequency dependency of small scale fading. The model is based on electromagnetic diffraction mechanism, which is a major factor of frequency dependent fading in UWB systems, geometric theory of diffraction, and scattering center analysis. The statistical distribution of model parameters can be easily estimated for any site specific measurements. The Intel channel measurements [14] are used to demonstrate the effectiveness and robustness of the novel model.**

***Index Terms*— Ultra-Wideband, Channel Model, Frequency Dependency, Geometrical Theory of Diffraction (GTD), Turin Model**

I. Introduction

ULTRA-Wideband (UWB) technology is rapidly shaping up as a potential solution to a variety of short-range problems, such as accurate ranging and positioning as well as indoor wireless networks [1-3]. However, ultra-wideband nature of UWB signal brings new challenges both in the analysis and practice of reliable systems. One of the key challenges is to build reliable UWB channel models for helping to predict system performance as well as optimize the physical layer design. Because of ultra-wideband nature of UWB signal, the UWB channel is regarded as frequency selective. Most proposed models [4-10] are simply a extensions of wideband impulse response model [11], a stationary linear filter [12-13]. However, based on the measurements from various working environments [14], UWB channel has a distinct characteristic: the physical environment has a much more significant impact on the time dispersive nature of the channel than in distance. Unfortunately, traditional statistical simulation models can not be easily changed for different environments and often require further measurements; moreover, reconstruction results show that traditional channel models produce large error (more than 15%) at each frequency point as signal bandwidth increases to 6 GHz. Originating from UWB radar scattering analysis, we believe that such large errors are caused because frequency dependency is not included in traditional models [15-16]. Frequency dependency is a site-specific information resulting from electromagnetic diffraction mechanism and causing the field strength to vary with the frequency in each ray. In the UWB large scale fading model, the frequency dependency has been identified for path loss calculation. However, for small scale fading, diffraction mechanism still needs to be considered for causing frequency dependency effect in order to obtain more accurate models.

In this paper, focusing on small-scale fading, a parametric UWB channel model, incorporating frequency dependency of each ray, is proposed. Both traditional Turin [12-13] and novel UWB channel models are thoroughly described. We also employ efficient subspace-based methods [17] to reconstruct the channel from practical measurements. Compared with traditional models, the proposed model gives much better fit to measured data. This model, originating from GTD based scattering analysis, is also more suitable for estimating frequency dependence coefficients.

II. UWB Traditional Small Scale Channel Model

The time-invariant impulse response of a UWB multipath fading channel can be written as:

$$h(t) = \sum_{\ell=1}^{L} a_\ell \delta(t - \tau_\ell) e^{j\theta_\ell} \tag{1}$$

where t is the observation time, L is the number of multipath components, $\{a_\ell, \tau_\ell, \theta_\ell\}$ are the random amplitude, arrival-time, and phase sequence of each path respectively and δ is the Dirac delta function. Furthermore, all unknown parameters, $\{a_\ell, \tau_\ell, \theta_\ell\}$, can be estimated using an efficient closed-form solution if we consider the problem in the frequency domain. Let $H(w)$ denote the Fourier transform of $h(t)$:

$$H(w) = \sum_{\ell=1}^{L} a_\ell e^{-jw\tau_\ell}. \tag{2}$$

Now, the unknown time delays appear as complex frequencies while propagation coefficients appear as unknown weights. Therefore, by considering the frequency domain representation of UWB channel, we have converted the problem of estimating the unknown channel parameters into classical harmonic retrieval problem, which is commonly encountered in spectral estimation.

Model (1) and (2) are known as the Turin model [12-13], which is widely adopted for UWB channel modelling.

National ICT Australia is funded by the Australian Government's Department of Communications, Information Technology and the Arts and the Australian Research Council through Backing Australia's Ability and the ICT Centre of Excellence program.

T.D. Abhayapala and Jian Zhang are also with the Research School of Information Science and Engineering, Australian National University.

Then, the modelling of the UWB wireless channel reduces to find statistical distribution for each parameter, which greatly depends on physical environment. A large number of measurement campaigns and channel modelling efforts have been carried out to characterize the UWB channel; and many kinds of parameter distribution with different values have been proposed until now. Among these models, the well-known Saleh-Valenzuela (S-V) indoor channel model [18] has been modified and adopted by IEEE 802.15.3a standard [14]. In the S-V model, multipath components arrive at the receiver in groups (clusters). Both cluster arrivals and subsequent arrivals within each cluster are Poisson distributed. The amplitude of each ray are assumed to have independent log-normal distribution.

However, the distinct disadvantage of this type of models is that they are not easy to change for different environments in which various kinds of UWB devices will be operating, as no environmental specific parameters are incorporated. Further measurements are also required to obtain accurate parameter distributions. Moreover, reconstruction results show that traditional channel models produce larger error (15% [1]) as signal bandwidth increases to 6GHz.

III. Proposed Ultra-Wideband Channel Model with Frequency Dependence

Our aim is to develop a novel UWB channel model to categorize real environments into several classes and extract the relevant parameters in direct comparison with measured data. Originating from radar scattering analysis, we build a new model by incorporating frequency dependency of the individual rays as an input. Frequency-dependency, arising from electromagnetic diffraction mechanism, causes the field strength to vary with the frequency in each ray [15-16]. For narrowband signals, the frequency-dependent features of each individual ray path are small and become negligible. However, when it comes to broadband systems, especially UWB, the frequency dependent feature should be considered. Unfortunately, none of rays in Turin's model has frequency dependence. The physics of frequency dependence and Geometric Theory of Diffraction (GTD) based UWB channel model are introduced below.

A. Physical Mechanism of Channel Modelling

In this section, we introduce one of the mechanism causing the frequency dependency of the individual path by investigating the electromagnetic wave propagation. Now, to characterize the radio propagation, we consider a general environment of multiple reflections, transmissions, and diffractions (Fig. 1). Here we assume that all scatters are located in a circle, or close to the scattering origin. Let the incident field on an object, located on $\mathbf{r}$, is due to a plan wave transmitting in the $+\mathbf{z}$ direction, where $+\mathbf{z}$ denotes an unit vector with respect to the origin. The field strength at location $\mathbf{r}$ can be described by

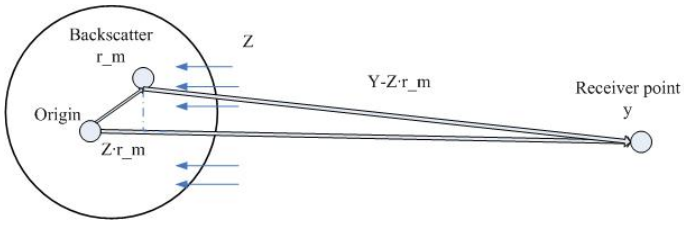

Fig. 1. Physical mechanism of radio propagation

$$E(\underline{\mathbf{r}}) = E_0 e^{-jk\mathbf{z}\cdot\mathbf{r}} \tag{3}$$

where $k = 2\pi/\lambda$, or $k = w/c$, is the wavenumber, $j = \sqrt{-1}$, λ is the wavelength, c is the speed of wave propagation and E_0 is the field strength at the origin. From the geometrical theory of diffraction [19], when the wavelength is small compared with the object, the backscattered field at a point $\mathbf{y}$ appears like a set of discrete scattering centers and can be approximated by

$$E(k, y) \approx \frac{E_0}{|\mathbf{y}|} e^{jk\mathbf{y}} \sum_{m=1}^{M} \phi_{m,k} e^{-j2k\mathbf{z}\cdot\mathbf{r_m}} \tag{4}$$

where $\mathbf{r_m}$ is the location of the mth scattering center, and $\phi_{m,k}$ is a frequency dependent factor determined by the scattering mechanism. Here the approximation $|\mathbf{y} - \mathbf{z}\cdot\mathbf{r_m}| = \mathbf{y}$ is made by assuming farfield backscatter.

From radar scattering analysis [15-16], among three typical propagation mechanisms: line of sight (LOS), reflection, and diffraction, only diffraction causes the strength to be frequency dependent. Moreover, the GTD predicts the scattering follows $(jk)^\alpha$ frequency dependency, where α is an integer multiple of $1/2$. Hence, the field strength for wavenumber k is represented by the following model:

$$E(k) = \sum_{m=1}^{M} A_m (j\frac{k}{k_0})^{\alpha_m} e^{-j2k|\mathbf{r_m}|}. \tag{5}$$

Here, k_0 is the lowest wavenumber; the frequency dependence factor α_m is determined by the geometric configurations of the objects as listed in Table 1. Note that $|\mathbf{r_m}| = \mathbf{z}\cdot\mathbf{r_m}$, which gives the range of all scatters with respect to a zero-phase reference.

The model parameters $\{A_m, \alpha_m, \mathbf{r_m}\}$ characterize the M individual scattering centers. Especially, in [20], the frequency dependence factor in (5) is used for channel modelling. Therefore, by tracing the frequency dependence of each ray, we can get more insights into the propagation features of a specific channel.

B. GTD-based Modified UWB channel model

Now, to better characterize the ray path, we propose a modified model to incorporate the frequency dependency described above. As wavenumber $k = w/c$, the modified model has

[1] In reconstruction stage, both original and reconstructed channel impulse responses are normalized for comparison. 15% errors means that there are 0.15 units difference at each frequency point.

Physical Mechanism	Frequency Dependence Factor α
Line of Sight	0
Reflection	0
Diffraction from smooth or flat surface	0
Diffraction by edge	-0.5
Diffraction by Corner or tip	-1
Diffraction by Axial Cylinder Face	+0.5
Diffraction by Broadside of a Cylinder	+1

TABLE I

PHYSICAL MECHANISM VERSUS FREQUENCY DEPENDENCE w^{α} [19]

frequency dependence factor $(w/w_0)^{\alpha}$, where w_0 is the lowest angular frequency. Note here $(w/w_0)^{\alpha}$, instead of w^{α}, is used to account for frequency dependence effect. This is because according to practical measurements, frequency dependency just has a little impact on channel impulse response. Moreover, the frequency dependence coefficients α for each ray, rely on ray path physical mechanisms like diffraction, reflection, and LOS, and geometric configurations.

Therefore, we write the impulse response of the modified multipath fading channel in the frequency domain as:

$$H(w) = \sum_{\ell=1}^{L} a_{\ell} \left(\frac{w}{w_0}\right)^{\alpha_{\ell}} e^{-jw\tau_{\ell}} \tag{6}$$

where L versions of the transmitted signal are assumed to be received, $\{a_{\ell}, \tau_{\ell}\}$ are still the random amplitude and the time delay of each ray. Frequency dependence $(w/w_0)^{\alpha}$ of common value have been listed in Table 1. Note that for narrowband systems, the frequency dependency can be neglected, as w is close to w_0, thus the frequency dependence factor is always equal to 1.

For a given environment, a set of channel sounding measurements can be used with any efficient subspace-based method to estimate parameters $\{a_{\ell}, \alpha_{\ell}, \tau_{\ell}\}$. In this paper, we use Intel measurements [14] to resolve these parameters as an example. The reconstruction results show that our GTD based modified model gives good results for channel reconstruction, with error of less than 10%.

IV. EXAMPLE: CHANNEL RECONSTRUCTION AND COMPARISON

A. Methodology

In this section, we use well studied high-resolution harmonic retrieval methods to obtain estimation for the unknown parameters of both UWB channel models: (i) Turin and (ii) GTD based modified models. In the following, we will adopt the subspace-based approach [17] to estimate the Turin and GTD based modified models, and show that it is possible to obtain high-resolution estimates of all the relevant parameters. The algorithms are described in Appendix .

Intel research measurements $H(w)$ from 2-8 GHz in residential environments will be used as channel impulse response in frequency domain [14]. The measurements are taken with 1601 samples for frequency between 2 and 8 GHz, with a frequency spacing of 3.75MHz. Processing has already been performed on this data to isolate channel response from any other component in the system, such as gain stages, cabling, antennas, etc.

B. Channel Reconstruction Results

The channel reconstruction is performed on 6 GHz bandwidth and compared with original channel frequency impulse response, as shown in Figure 2-3. According to figures, it is shown that the traditional Turin model produces larger deviation between reconstructed and original impulse response. Moreover, in Figure 3 , we see that the GTD modified model could give good fit for both low and high frequency parts. It is concluded that novel model could give faster and more accurate fit for high frequency UWB systems.

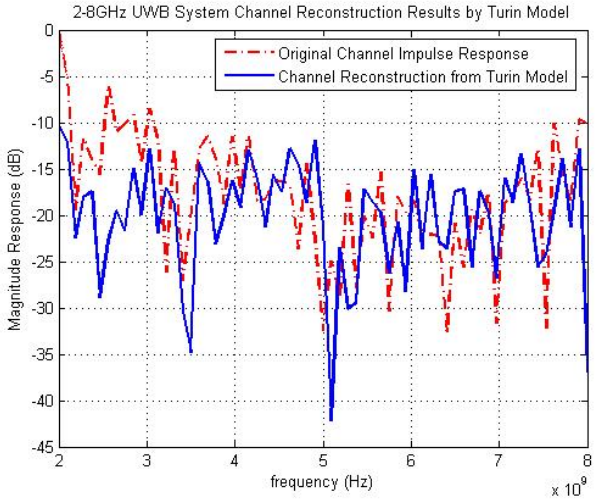

Fig. 2. 6 GHz UWB channel reconstruction results from Turin Model

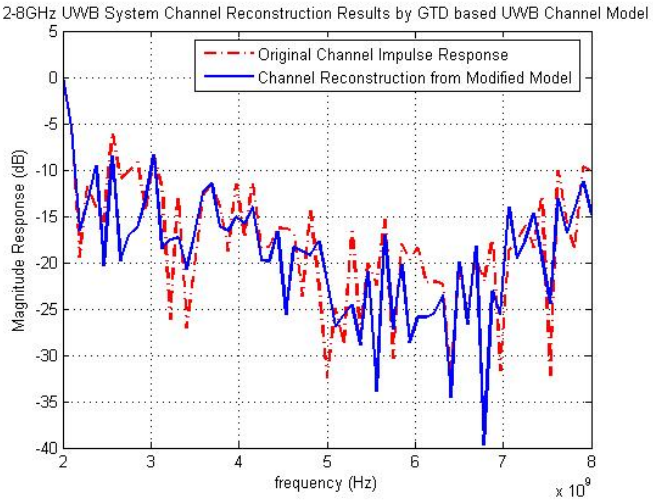

Fig. 3. 6 GHz UWB channel reconstruction results from GTD based channel model

In order to make the comparison more clear, the difference between reconstructed and original channel impulse response

at each frequency point is shown in Figure 4 for comparison of these two models in townhouse environment. Note that according to above algorithms, we have 354 multipaths for Turin model and GTD based model. From the reconstruction results, it can be seen that the novel UWB channel model with frequency dependence provides much more accurate fit (with error less than 10% for 6GHz bandwidth). The traditional Turin model could give good fit to narrowband (with error of $0.8e^{-13}\%$ for 750MHz bandwidth); but, when it comes to super wideband, there are significant error (for example, more than 16% for 6GHz bandwidth) between reconstructed and original channel impulse response. This results prove that frequency dependence needs to be considered for large bandwidth. Furthermore, considering office environments, quite similar results are shown when more number of multipaths are considered; in our cases, we have 535 multipaths.

Furthermore, from the reconstruction results, we observed that most paths undertake line-of-sight or reflection, which is frequency independent ($\alpha = 0$), or one time diffraction ($\alpha = -1/2$). This result is very reasonable in indoor environment.

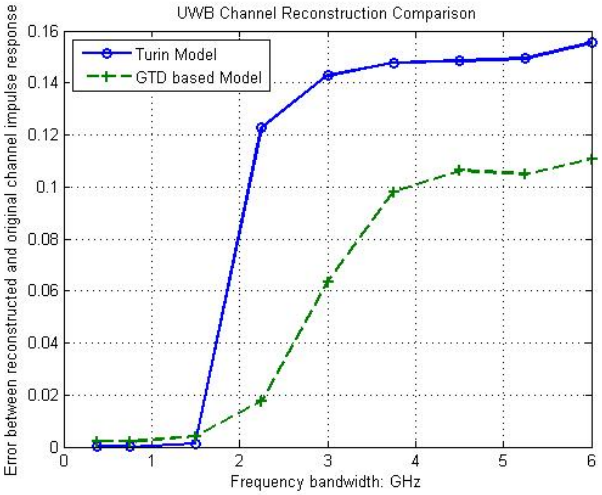

Fig. 4. UWB channel reconstruction error comparison via increasing bandwidth

V. Conclusion

A new theoretical framework for UWB channel modelling is established based on physical mechanism of wave propagation at different frequencies. A novel GTD based modified UWB channel model is proposed. Due to the improved frequency dependency of the model, it provides better fit to site specific data compared with traditional models.

References

[1] Liuqing Yang and G.B. Giannakis, "Ultra-Wideband Communications," *IEEE Signal Processing Magzine*, vol. 21, issue. 6, pp. 26-54, 2004.

[2] L. De Nardis, P. Baldai and M. G. Di Benedetto, "UWB ad-hoc networks," *IEEE Conference on UWB Systems and Technologies Digest of Papers*, Baltimore, Maryland, pp. 219-223, 2002.

[3] M. Ho, L. Taylor, and G. R. Aiello, "UWB technology for wireless video networking," *International Conference on Consumer Electronics*, Los Angeles, CA, pp. 18-19, June 2001.

[4] Z. Irahhauten, H. Nikookar, and G. J. M. Janssen, "An Overview of Ultra Wide Band Indoor Channel Measurements and Modeling," *IEEE Microwve and Wireless Componnets Letters*, vol. 14, no. 8, 2004.

[5] H. Lee, B. Han, Y. Shin, and S. Im, "Multipath Characteristics of Impulse Radio Channels," *IEEE VTS 51st Vehicular Technology Conference*, vol. 3, pp. 2487-2491, Spring 2000.

[6] J. R. Foerster, "The Effects of Multipath Interference on the Performance of UWB Systems in an Indoor Wireless Channel," *IEEE VTS 53rd Vehicular Technology Conference*, vol. 2, pp. 1176-1180, Spring 2001.

[7] F. Zhu, Z. Wu, and C. Nassar, "Generalized Fading Channel Model with Application to UWB," *IEEE Conference on Ultra Wideband Systems and Technology*, pp. 21-23, May. 2002.

[8] V. Hovinen, M. Hmlinen, and T. Ptsi, "Ultra Wideband Indoor Radio Channel Models: Preliminary Results," *IEEE Conference on Ultra Wideband Systems and Technology*, pp. 75-79, May. 2002.

[9] D. Cassioli, M Z. Win, and A. F. Molisch, "The Ultra-Wide Bandwidth Indoor Channel: From Statistical Model to Simulations," *IEEE Journal on Selected Areas in Communications*, vol. 20, issue. 6, pp. 1247-1257, Aug. 2002.

[10] H. Zhang, T. Udagawa, T. Arita, and M. Nakagawa, "A Statistical Model for the Small-Scale Multipath Fading Characteristics of Ultra Wideband Indoor Channel," *IEEE Conference on Ultra Wideband Systems and Technology*, pp. 81-85, May. 2002.

[11] T. S. Rappaport, *Wireless Communications: Principles and Pratice* Upper Saddle River, NJ: Prentice Hall, 1996.

[12] H. Hashemi, "The Indoor Radio Propagation Channel," *Proc. IEEE*, vol. 81, no. 7, pp. 941-968, 1993.

[13] K. Pahalanvan and A. H. Levesque, *Wireless Infromation Networks*, John Wiley and Sons, New York, 1995.

[14] J. Foerster and Qinghua, Li, "UWB Channel Modeling Contribution from Intel," IEEE P802.15 Wireless Personal Area Network, 2002.

[15] C.A. Balanis, *Advanced Engieering Electromagnetics*, John Wiley and Sons, 1989.

[16] L.B. Felsen and N. Marcuvitz, *Marcuviz, Radiation and Scatering of Waves*, Pentice-Hall, New Jersey, 1973.

[17] Irena Maravic, "Sampling Methods for Parametric Non-Bandlimited Signals: Extensions and Applications," Thesis to University of California at Berkeley, 2004.

[18] A. A. M. Saleh and R. A. Valenzauela, "A statistical model for indoor multipath propagations," *IEEE J. Select. Areas Commun*, vol. 5, no. 2, pp. 128-137, 1987.

[19] L.C. Potter, D.M. Chiang, R. Carriere, and M.J. Ferry, "A GTD-based Parameter model for radar scattering," *IEEE Trans. Antennas Propagat.*, vol. 43, pp. 1058-1067, 1995.

[20] R. C. Qiu, "A Theoretical Study of the Ultra-wideband Wireless Propagation Channel Based on the Scattering Centers," *IEEE Journal on Selected Areas in Communications*, vol. 20, issue. 9, pp. 1628-1637, Dec. 2002.

Appendix

Subspace-based Method

From the set of samples $H(q)$ (Intel's measurements), the channel impulse response in frequency domain can be expressed as:

$$H(q) = H(w_0 + q * w_s) \tag{7}$$

where $w_s = B/Q - 1, q = 0, 1, ..., Q - 1$, w_0 is the lowest frequency in the whole bandwidth, w_s is the frequency spacing of each sampling. Q is the total sampling points. While in our channel reconstruction example, $w_0 = 2$ GHz, $w_s = 3.75$ MHz, and $Q = 1601$.

A. Channel Reconstruction by Turin Model

From Turin model, the samples of $H(q)$ can be expressed as a sum of complex exponential.

$$H(q) = \sum_{\ell=1}^{L} a_\ell e^{-j(w_0+qw_s)\tau_\ell} + N(q) = \sum_{\ell=1}^{L} \widetilde{a}_\ell e^{-jqw_s\tau_\ell} + N(q). \tag{8}$$

Note that White Gaussian Noise ($N(q)$) is considered here for channel reconstruction. Then, the sub-space techniques could be employed to estimate unknown parameters, time delay τ_ℓ and path amplitude a_ℓ. Applying such techniques to UWB systems would be possible and efficient by avoiding explicit computation of the covariance matrix. The algorithm is summarized as follows.

1. Given the set of coefficients $H(q)$, construct a Hankel data matrix H_s of size $P * V$, where $P, V > L$,

$$H_s = \begin{pmatrix} H_s(0) & H_s(1) & ... & H_s(V-1) \\ H_s(1) & H_s(2) & ... & H_s(V) \\ ... & & & \\ H_s(P-1) & H_s(P) & ... & H_s(P+V-2) \end{pmatrix}. \tag{9}$$

2. Compute the singular value decomposition of H_s

$$H_s = U_s \wedge_s V_s^H + U_n \wedge_n V_n^H \tag{10}$$

where the columns of U_s and V_s are L principle left and right singular vectors of H_s respectively. And U_s, $\wedge_s$ and V_s are

$$U_s = \begin{pmatrix} 1 & 1 & 1 & 1 & 1 \\ z_1 & z_2 & z_3 & ... & z_L \\ ... & & & & \\ z_1^{P-1} & z_2^{P-1} & z_3^{P-1} & ... & z_L^{P-1} \end{pmatrix} \tag{11}$$

$$\wedge_s = diag(\widetilde{a_1}\widetilde{a_2}\widetilde{a_3}...\widetilde{a_L}) \tag{12}$$

$$V_s = \begin{pmatrix} 1 & 1 & 1 & 1 & 1 \\ z_1 & z_2 & z_3 & ... & z_L \\ ... & & & & \\ z_1^{V-1} & z_2^{V-1} & z_3^{V-1} & ... & z_L^{V-1} \end{pmatrix}. \tag{13}$$

3. Estimate the signal poles $z_\ell = e^{-jw_s\tau_\ell}$ by computing the eigenvalues of a matrix Z

$$Z = \underline{U_s^+}\,\overline{U_s} \tag{14}$$

where $\underline{(\cdot)}$, $\overline{(\cdot)}$ denote the operating of omitting the first and the last row of $(\cdot)$ respectively; and $(\cdot)^+$ denotes the pseudo inverse of $(\cdot)$. Obviously, in the absence of noise, the signal poles can be perfectly estimated , in the presence of noise it is possible to estimate the time delays from L roots of $H(z)$ which are closest to the unit circle.

4. Find the coefficients $\widetilde{a_l}$ from the Vandermonde system, that is

$$H_s(q) = \sum_{\ell=1}^{L} \widetilde{a_\ell} e^{-jqw_s\tau_\ell} + N(q) \tag{15}$$

by fitting the L exponentials $e^{-jw_s\tau_l}$ to the data set.

B. Channel Reconstruction by Modified Channel Model

In the modified UWB channel model with frequency dependence, the same set of samples can be expressed as:

$$H(q) = \sum_{\ell=1}^{L} a_\ell (\frac{w_0 + qw_s}{w_0})^{\alpha_\ell} e^{-jqw_s\tau_\ell} + N(q). \tag{16}$$

As shown in Section III.A, α_ℓ is an integer multiple of 1/2. Therefore (16) can be written as:

$$H(q) = \sum_{\ell=1}^{L} \sum_{r=-(R-1)/2}^{(R-1)/2} C_{\ell,r} (\frac{w_0 + qw_s}{w_0})^{-r/2} e^{-jqw_s\tau_\ell} + N(q). \tag{17}$$

Here, R is an even integer. Obviously, we can use modified subspace-based method to estimate unknown parameters. The algorithm is concluded as follows:

1. Given the set of coefficients $H(q)$, construct a Hankel data matrix H_s of size $P * Q$, where $P, V > L$, same as (9).

2. Compute the singular value decomposition of H_s

$$H_s = U_s \wedge_s V_s^H + U_n \wedge_n V_n^H \tag{18}$$

where the columns of U_s and V_s are RL principle left and right singular vectors of H_s respectively.

3. Estimate the signal poles $z_\ell = e^{-jw_s\tau_\ell}$ by computing the eigenvalues of a matrix Z, defined as

$$Z = \underline{U_s^+}\,\overline{U_s}. \tag{19}$$

While in the noiseless case, we can find RL signal poles, each of multiplicity L; in the presence of noise it is desirable to estimate the time delays from L roots of $H(z)$ which are closest to the unit circle.

4. Solve the coefficients, a_ℓ and R (or α_ℓ), by solving the system of least-square equation, that is

$$H(q) = \sum_{l=1}^{L} \sum_{r=-(R-1)/2}^{(R-1)/2} C_{l,r} (\frac{w_l + qw_s}{w_l})^{-r/2} e^{-jqw_s\tau_l} + N(q) \tag{20}$$

by fitting the L exponentials $e^{-jw_s\tau_l}$ to the data set.